

Operationalizing the Arrow of Time in mesoscopic: A Unified Framework for Non-equilibrium Matter

Yikun Ren^{1*}, Feixiang Xu², Ming Lin¹

^{1*}School of Materials Science and Engineering, Jiujiang University, Jiujiang, 332005, Jiangxi, China.

²BYD Company Limited, Shenzhen, 518000, Guangdong, China.

*Corresponding author(s). E-mail(s): 6260004@jju.edu.cn;
Contributing authors: fxxusz@gmail.com; linmingzny@163.com;

Abstract:

What sustains a non-equilibrium system against fluctuations from within—as witnessed in non-equilibrium steady states, glassy relaxation, and even living organisms? Here we show that the arrow of time itself can be operationalized into a measurable physical quantity on mesoscopic particles—the eigen-phase displacement. This displacement gives rise to a non-local generalized force, the thermodynamic inertia force, which emerges from the integrated contribution of local constraints rather than as a conventional local force. It actively counteracts fluctuations and its algebraic structure is a semi-group, fundamentally distinct from the Lie group of Newton inertia, thereby encoding the irreversibility of time’s arrow. Building on this foundation, we construct a unified Microstate-Sequence—Mode-Coupling (MSS-MCT) theory. Its thermodynamic limit is defined by Microstate Sequence (MSS) theory, and its dynamical action is captured by a consequent mode-coupling theory (MCT). From this single first-principles framework, we simultaneously resolve two long-standing puzzles: it predicts the giant non-Gaussian parameter(1~10), closing the order-of-magnitude gap with experiments that standard mode-coupling theory could not explain; and it delivers a first-principles, non-fitting derivation of the universal polymer constant $C_1 \approx 16.7$ with merely 1% error — the most accurate theoretical prediction to date, dramatically surpassing the Adam-Gibbs(>100%) and others(>200%). Our work establishes thermodynamic inertia as a foundational principle for non-equilibrium matter, bridging thermodynamic and dynamic descriptions from glassy relaxation to the maintenance of life.

Introduction:

Within the system, what force enables a living cell to repair itself, or a supercooled liquid to resist crystallization? Beneath these disparate phenomena lies a unified physical question: how can a non-equilibrium system actively oppose the thermal fluctuations that constantly drive it toward equilibrium within itself? We observe such spontaneous fluctuation-resistance vividly in polymer systems, small particle glassy systems and living systems: the phase space of glassy systems exhibits broken ergodicity¹⁻³; the time-integral of random forces on particles in non-equilibrium systems does not vanish^{4,5}, indicating a persistent directed influence; and profound paradoxes such as the Kauzmann entropy crisis persist^{6,7}; the immortal Henrietta Lacks cells⁸. Yet, even Onsager and Prigogine’s mesoscopic framework⁹⁻¹¹, which correctly establishes the thermodynamic possibility of non-equilibrium steady states, does not specify the mesoscopic mechanism that internally enforces the stability of the eigen-phase. Here we argue that the answer resides in the most fundamental yet under-utilized concept in physics: the arrow of time¹²⁻¹⁸. (While the ultimate

physical origin of the arrow remains debated, its reality as the source of entropic driving is unquestioned¹⁹⁻²¹; our aim is not to enter that foundational debate but to operationalize the concept for solving concrete physical problems.) We build the Microstate-Sequence-Mode-Coupling (MSS-MCT) theory to operationalized the arrow of time into a concrete physical force and proved its correctness by solving puzzles of decades in different regions and different structural systems.

This concrete force becomes strikingly visible in two classic, unsolved problems that span the thermodynamic and dynamic descriptions of non-equilibrium matter. On the dynamic side, the large non-Gaussian parameter α_2 (typically 1–10)²²⁻²⁵ observed in glassy relaxation presents an order-of-magnitude discrepancy with predictions of standard mode-coupling theory (MCT). In the glass-transition region, experiments consistently observe α_2 deviating significantly from zero, typically in the range of 1–10, indicating strongly non-Gaussian particle-displacement distributions and pronounced dynamic heterogeneity. However, mode-coupling theory (MCT) based on near-equilibrium assumptions predicts an α_2 value close to 0.1—an order-of-magnitude gap from the experimental reality²⁴⁻²⁶. It is important to note that MCT’s explanation of the local “cage effect” is profound and correct²⁷. Within MCT, particles can be roughly divided into those trapped by the cage effect and those that escape. Although the confinement arising from structural “tightness” is strong enough, the dynamical difference between these two populations remains insufficient to produce a large non-Gaussian parameter, yielding only about 0.1. This discrepancy strongly hints at a global driving mechanism beyond the local “cage effect” that continuously reshapes dynamical correlations among particles. The failure of the standard MCT stems fundamentally from its treatment of fluctuations. At equilibrium, the time integral of the random force acting on a mesoscopic particle collective vanishes, rendering fluctuations purely dissipative²⁸. In contrast, within a non-equilibrium phase or even far-from-equilibrium state, the time-averaged random force corresponding to the collective motion of mesoscopic particles does not vanish — a definitive statistical signature of a non-equilibrium state, as established by fluctuation theorems including Jarzynski²⁹, Crooks³⁰ and so on^{31,32}. This key observation reveals the presence of a persistent, directed driving force intertwined with stochastic noise. Consequently, a complete theory of non-equilibrium dynamics must provide a framework to mathematically disentangle this directed drive from pure random fluctuations—a first-principle origin of mesoscopics.

On the thermodynamic side, the universal constant $C_1 \approx 16.7$ in the Williams–Landel–Ferry equation—a cornerstone of polymer glass transition—has resisted first-principles explanation for seven decades^{7,33-35}. Although the concept of “free volume” proposed by Flory to explain this universality has long been recognized as fundamentally flawed^{6,24,36}, the experimental universality of C_1 —its independence from polymer chemical structure and cooling history—reveals a hidden, structure-independent statistical-mechanical mechanism³⁷. Nevertheless, all mainstream theories based on equilibrium or near-equilibrium assumptions—whether Simha-Boyer’s vibrational volume model³⁸, Cohen-Grest’s Lennard-Jones potential theory^{35,39}, or Adam-Gibbs’s CRR and configurational entropy⁴⁰⁻⁴³—fail dramatically when attempting first-principles calculations of C_1 , with errors exceeding 100–300%. This systematic failure indicates the existence of a strict thermodynamic mechanism that does not rely on “free volume” as a reference and does not rest on near-equilibrium assumptions. All attempts rooted in “free-volume” or equilibrium-based models yield errors exceeding 100 %. These two puzzles represent a deep schism: one originates in thermodynamics, the other in dynamics, and neither has been resolved from a common,

first-principles origin of mesoscopies.

In order to solve the puzzles, we have extended Prigogine's "first-principles thinking"^{44,45} in thermodynamics. Our approach unfolds in three steps. First, using number-theoretic methods, we arrange all possible system states into a sequence that varies continuously across all structural and energetic parameters. The second law of thermodynamics then dictates that a truncated subsequence of this arrangement constitutes the non-equilibrium eigen-phase. This fusion of number theory and thermodynamics forms the Microstate Sequence (MSS) theory⁴⁶. Then, extracting a rigorous mathematical expression for the eigen-phase from MSS theory to define the thermodynamic inertia force. Crucially, this force obeys a semigroup algebra, lacking the inverse elements characteristic of classical mechanical forces; this mathematical structure directly encodes the irreversibility of time. Second, this force is involved into the Liouville equation and, via the Mori-Zwanzig projection operator formalism^{47,48}, to derive a new Mode-Coupling Theory (MCT) equation. Unifying the MSS and MCT equations yields the closed MSS-MCT equations. Finally, we apply this coupled framework to systems with different structures. As a result, we obtain the two key parameters to prove the thermodynamic inertia force—non-gaussian parameter (10 times larger than NMCT predicted, $\alpha_2 \in (1,10)$) and the C1 in Flory's conjecture (non-fitting way to get 16.7, with merely 1% error margin less than Adam-Gibbs theory's 100%). Finally, we discuss the conceptual relationships between MSS-MCT theory, Replica Theory⁴⁹, and Mode-Coupling Theory⁵⁰.

I. Foundation of eigen-phase displacement theory

1.1 Theoretical Assumptions and Framework

We begin by presenting a description of the system as a whole. A system far from equilibrium undergoes complex temporal evolution of its microstates within phase space. However, if the pure dissipative fluctuations are removed—or if one observes only the center of fluctuations—then, in principle, no violation of the second law can be detected within finite spacetime. We define the statistical ensemble corresponding to the “stationary” average at the center of fluctuations as the system’s eigen-phase. It represents a probability-weighted collection of all possible microstates under given external constraints. Building upon the instantaneous and universal nature of the arrow of time, our theory of non-equilibrium thermodynamics is founded on the following basic Thermodynamic Law concerning the arrow of time and eigen-phase:

Law of Arrow of Time and Eigen-Phase:

The eigen-phase is the direct manifestation of the arrow of time in a non-equilibrium system; it is the center of fluctuations. For a nonequilibrium system, the thermodynamical structure of the eigen-phase are determined by the second law of thermodynamics through the following variational statement:

$$\delta(S(\text{eigen-phase})) + \int dS_e = \delta(-k \sum_i P_i \ln P_i + \int dS_e) = 0 \quad (1)$$

In the equation (1), the dS_e/dt is the external entropy flux, $S(\text{eigen-phase})$ is the entropy of eigen-phase, P is the thermal probability of microstate i . This law establishes the eigen-phase as the statistically "most probable" distribution and identifies its physical origin. From within the non-equilibrium system, the law continuously drives a probability current at every point and every

moment. Its net effect is to shape and sustain this maximum-entropy probability distribution—the eigen-phase—thereby rendering it the “attractor” of the system’s evolution. The scheme of the eigen-phase “balance” could be shown in figure 1:

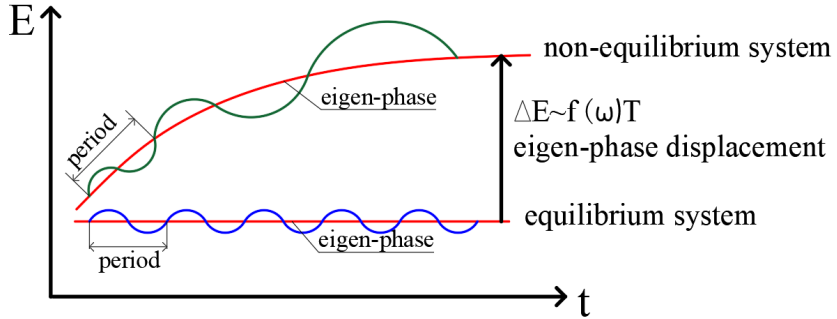


Figure 1. The fluctuation center manifests of equilibrium and non-equilibrium systems. The red line represents the fluctuation centers for equilibrium and non-equilibrium systems. The fluctuation center, fluctuation amplitude, and relaxation time of an equilibrium system remain constant. In contrast, the fluctuation center of the non-equilibrium system is displaced away from that of the equilibrium system, and both its fluctuation amplitude and relaxation time undergo changes. Due to fluctuations, an isolated non-equilibrium system will inevitably evolve toward equilibrium, but the process is typically much slower than predicted by dynamics alone. This is because the eigen-phase displacement, as illustrated in the figure, actively pushes particles in Mean Areas(defined in the following paragraph) that have deviated from the non-equilibrium eigen-phase back toward it, thereby retarding the relaxation process. This is the essence of thermodynamic inertia, or equivalently, a thermodynamic memory effect.

As illustrated in Figure 1, the essential distinction between non-equilibrium and equilibrium systems lies in the time-dependent nature of the non-equilibrium eigen-phase. Constrained by the second law of thermodynamics, the eigen-phase of a non-equilibrium system must satisfy the condition that:

$$\Delta E = \langle E \rangle_{ne} - \langle E \rangle_{eq} \sim f(\omega) T, f(\omega) T - T \int_t^{t+\Delta t} J dt \geq 0 \quad (2)$$

Defining F as free energy, and $f(\omega)$ as the self-driving conservative force, ω is the degree of non-equilibrium which would be clearly defined later, $\langle E \rangle_{eq}$ is the ensemble-averaged energy of equilibrium system, $\langle E \rangle_{ne}$ is the ensemble-averaged energy of non-equilibrium system placed, J is external entropy flux $J = \frac{dS_e}{dt}$, eigen-phase energy differential ΔE is the the energy differential between non-equilibrium and equilibrium ensemble averages which could be used to define the eigen-phase displacement.

Next, we proceed to precisely define the mesoscopic level adopted in this work. The local equilibrium hypothesis, as formulated by Prigogine, has been used to solve near-from-equilibrium systems. To describe more complex non-equilibrium systems like far-from-equilibrium systems, this framework requires extension⁵¹⁻⁵⁴. Building upon Prigogine’s theory, we establish a new mesoscopic scale larger than the local scale of Prigogine. This larger mesoscopic scale is defined as follows: As we gradually zoom in from the macroscopic scale to the microscopic scale, there always exists a particular mesoscopic scale, denoted as the Mean Area (MA). When the

observation scale is above the MA, the observer cannot detect dynamic heterogeneities but can observe the macroscopic statistical behavior of the system within a relatively short period of time. Conversely, when the observation scale is below the MA, the observer can detect dynamic heterogeneities but must observe over a longer period of time to grasp the macroscopic statistical behavior of the system. To provide a more rigorous mathematical and physical definition, based on the Local Assumption(Prigogine), we coarse-grain both the MA and the locale into N averaged particles (hereinafter referred to as "N-coarse-grained", where N is sufficiently large). The intersection of the sets of microstates of all locales is always contained within the set of microstates of the Mean Area (MA), and simultaneously, the set of microstates of the MA is always contained within the union of the sets of microstates of all locales. According to the definition of Mean Area, the mathematical definition of the Mean Area can be stated as: "The set of microstates of the coarse-grained MA is equal to the intersection of the sets of microstates of all coarse-grained locales" as shown in Equation (3).

$$\{\text{microstates in CG_MA}\} = \bigcap_{\text{locale} \subseteq \text{MA}} \{\text{microstates in CG_local}\} \quad (3)$$

By combining Equation (3) with the Local Assumption, it can be inferred that the N-coarse-grained Mean Area formally satisfies the partition function law. Without changing the degree of non-equilibrium, based on the second law of thermodynamics, the entropy of the CG_Mean Area could be regarded as "relatively equilibrium" if the locales are "small equilibrium systems". This is because, if the CG_Mean Area does not reach relative equilibrium without changing the degree of non-equilibrium, then CG-MA should be able to spontaneously relax towards any local. At a new moment, the new Spin generated in CG-MA will inevitably belong to a Spin that originally belonged only to a certain local, which violates equation (3). Therefore, a CG-MA that satisfies equation (3) will inevitably satisfy equation (1).

Consequently, the energy of a MA at any given time t and position x can be decomposed as follows, where δ and $\Delta E(x,t)$ represents the fluctuations and eigen-phase displacement, as shown in Equation (4) and (5).

$$E(x,t) = \langle E(x,t) \rangle_{\text{ne}} + \delta = \langle E \rangle_{\text{eq}} + \Delta E(x,t) + \delta \quad (4)$$

$$\Delta E(x,t) = \langle E(x,t) \rangle_{\text{ne}} - \langle E \rangle_{\text{eq}} \quad (5)$$

1.2 The first part of thermodynamic inertia theory: MSS

From the arrow of time, it can be inferred that all states of the eigen-phases of any isolated system gradually increase in sequence, eventually reaching equilibrium. Therefore, decomposing the set of microstates of an equilibrium system into such a sequence, arranged in the order given by the arrow of time, can clearly reflect the changing of the set of non-equilibrium microstates. So, microstate sequence theory(MSS, briefly explained in SI A) is such a statistical theory built for calculation of eigen-phase¹³. Using the number-theoretical approaches and the second law of thermodynamics, MSS arrange all microstates in a continuous and monotonic sequence in order of energy or other non-equilibrium indices(e.g. in 3D Ising model, the index of any microstate is strictly written in the function of numbers of +1 spin-spin couplings and distance between neighbored +1). It is important to note that MSS is a descriptive framework for eigen-phase trajectory, not a complete representation of the system's true phase trajectories. MSS does not capture fluctuations or metastates specifically, but it can still reflect statistical regularities in

non-equilibrium systems because it captures the eigen-phase. Using MSS theory and equation (2), here is the MSS CUTTING theorem:

All microstates of an eigen-phase of a Mean Area(MA) with certain energy always form a contiguous subsequence within the Microstate Sequence(MSS)(The detailed deduction of MSS cutting theorem and exact expression of MSS in Ising model could be seen in SI A):

$$P_i = \begin{cases} \frac{e^{-\beta E(i)}}{Z_{ne}} = \frac{e^{-\beta E(i)}}{\sum_{j=1}^{i_{max}} e^{-\beta E(j)}}, & 1 \leq i \leq i_{max} \\ 0, & i > i_{max} \end{cases} \quad (8)$$

$$\{\text{microstates' index in MSS cutting}\} = \{1, 2, 3, \dots, i_{max}\} \quad (9)$$

The MSS Cutting Theorem gives explicit form to the non-equilibrium eigen-phase through a precise number-theoretic truncation procedure. **It breaks the ergodic hypothesis, yet restores ergodicity when the system reaches equilibrium.** As an extension of the second law of thermodynamics under the Law of Arrow of Time and Eigen-Phase, the theorem is important for understanding the thermodynamic behavior of non-equilibrium systems.

Through MSS CUTTING Theorem, the microstates contained in the intrinsic phase of non-equilibrium systems can be achieved by “cutting” the MSS as shown in example of 4 spins Ising model in the following figure:

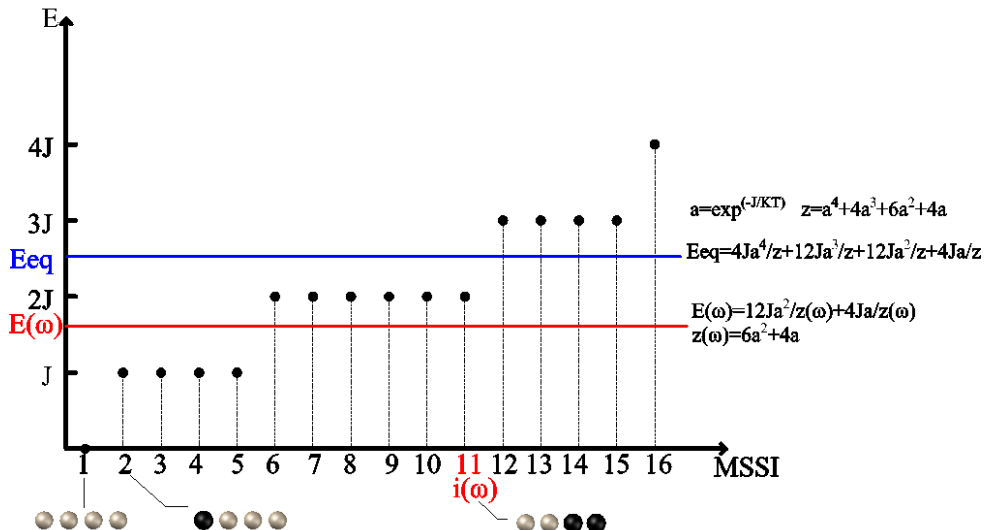


Figure 2. The energies of the different microstate sequences of the Ising system with four spins. MSSI is microstate sequence index. The X-axis represents the sequence of microstates ordered by their index within the MSS. The Y-axis represents energy. The horizontal blue line denotes the system energy at equilibrium, where the intrinsic phase encompasses all microstates. The horizontal red line indicates the energy of the non-equilibrium system at a non-equilibrium degree ω . In this state, the system includes only microstates corresponding to and to the left of the red line.

From Fig.2, we can see that the microstate set of non-equilibrium systems only needs to focus on the initial microstate and the final microstate because the property of MSS. By combining Equations (8) and (9), the degree of non-equilibrium and eigen-phase displacement should be:

$$\omega = \frac{W}{i_{max}} \quad (10)$$

$$r = e^{\Delta E/kT} = \frac{\sum_{i=1}^{W/\omega} e^{-E(i)/kT} / (W/\omega)}{\sum_{i=1}^W e^{-E(i)/kT} / W} = \frac{\overline{P}_{ne}}{\overline{P}_{eq}} \quad (11)$$

W is the number of microstates of a reference system (the equilibrium system is the first reference system), and i_{max} represents both the maximum sequence number of microstates and the

total number of microstates in the eigen phase. ω is the degree of non-equilibrium, which represents the degree of non-ergodicity of the whole system. E is the energy of microstate i . r represents the degree of non-ergodicity. P_{ne} is the probability of a single particle choosing to be “non-equilibrium states”. And P_{eq} is the probability of a single particle choosing to be “equilibrium states”. Therefore, r also means the probability change for an equivalent mean single particle caused by the degree of non-equilibrium. Because it comes from the MSS cutting which origin in second law of thermodynamics, and we will see in the formulas of MCT that the r is the “generalized-force” **which drive the particles back to the non-equilibrium eigen-phase**. So, r is defined as the eigen-phase displacement. Note that the effect of fluctuations is to cause individual particles to deviate from their deterministic trajectories, enabling them to sample all possible states and thereby approach equilibrium. The second law of thermodynamics dictates that the role of the eigen-phase displacement is to restore an equilibrated particle back to the non-equilibrium eigen-phase. Therefore, the eigen-phase displacement and fluctuations represent opposing yet complementary mechanisms in the balancing mechanism within non-equilibrium, collectively shaping the thermodynamic and dynamic behaviors of non-equilibrium systems. If the vital force in living systems is what sustains the “living state,” then its thermodynamic essence is none other than eigen-phase displacement. It is noteworthy that many non-equilibrium systems exhibit a highly heterogeneous distribution in their degree of non-equilibrium(5papers). A prominent example is dendritic segregation, which highlights the need to introduce a well-defined mesoscopic measure of the degree of non-equilibrium in order to properly capture its spatial heterogeneity. Furthermore, a clear mesoscopic conceptualization helps to clarify whether thermodynamic inertia is fundamentally a property of individual particles or an emergent collective property of particle assemblies.

The thermodynamic inertia force field originates from each Mean Area (MA) that is out of equilibrium, acting as a field source. This field drives the collective motion of particles both within and in the vicinity of the MA, thereby sustaining the non-equilibrium state. In our formulation, we first treat MAs as points distributed throughout the system. As field sources, they satisfy the following condition:

According to the definition of MA, we assume that the system consists of n MAs, each with volume dV , spatial coordinate x , and i_{max} microstates. We get:

$$\omega = \prod_x \omega(x) = \prod_x W^{dV/V} / i_{max}(x) = W / \prod_x i_{max}(x) \quad (12)$$

Equation (12) explains the collective of degrees of non-equilibrium of each MA and the total degree of non-equilibrium.

$$\omega(x) = W^{dV/V} / i_{max}(x) \quad (13)$$

Equation (13) describes the degree of non-equilibrium of the MA with its central position at point of x , subscript s means the “source”.

$$r = e^{\Delta E / kT} = \frac{\sum_{i=1}^{W / \prod_x i_{max}(x)} e^{-E(i)/kT} / (W / \prod_x i_{max}(x))}{\sum_{i=1}^W e^{-E(i)/kT} / W} = \prod_s r_s(x) \quad (14)$$

Equation (14) explains the collective of eigen-phase displacements of each MA source and the total eigen-phase displacement.

$$r_s(x) = e^{\Delta E(x) / kT} = \frac{\sum_{i=1}^{W^{dV/V} / \omega(x)} e^{-E(i)/kT} / (W^{dV/V} / \omega(x))}{\sum_{i=1}^{W^{dV/V}} e^{-E(i)/kT} / W^{dV/V}} \approx \frac{\overline{P_{ne}}}{\overline{P_{eq}}} \quad (15)$$

Equation (15) describes the eigen-phase displacement of the MA with its central position at point of x . The coupling of MA at x and MA at y should be:

$$r_s(xy) = e^{(\Delta E(x) + \Delta E(y)) / 2kT} \quad (16)$$

We then consider each MA as a spatial volume element, dV , within which all mesoscopic particles are subject to the thermodynamic inertia force. Given that the thermodynamic inertia force experienced by mesoscopic particles within a volume element dV becomes effectively indistinguishable when dV is sufficiently small, we apply the physical principle that “indistinguishability implies a uniform average.” Therefore, the eigen-phase displacement function for a particle located at a position y , with $y-x=\epsilon$ relative to the center x of an MA, is given by:

$$r(x+\epsilon) = \begin{cases} r_s(x)/2\epsilon & 0 < \epsilon \leq 0 \\ 1, \epsilon > 0 \end{cases} \quad (17)$$

$$\ln r(q) = \sum_x \ln r(x) (\theta(x+\epsilon) - \theta(x-\epsilon)) e^{-iqx} \delta(x) \quad (18)$$

Equation (16) describes the degree of non-equilibrium of the MA with its central position at point of x . $\theta(x)$ is the Heaviside step function. Owing to this generalized non-local interaction, it can be inferred that the emergence of Cooperatively Rearranging Regions (CRR) of Adam-Gibbs theory⁴⁰⁻⁴³ is a necessary consequence, although a detailed discussion of this point lies beyond the scope of the present paper. The last important parameter is the eigen-phase displacement heterogeneity $a(t)$, which means the potential field caused by the inertia force:

$$a(t) = \sum_{\epsilon \neq 0} \left. \frac{\partial \ln r(x+\epsilon)}{\partial y} \right|_{y=x+\epsilon} = \sum_i \frac{\partial \ln r(x+\epsilon)}{\partial \epsilon} \quad (19)$$

The integration of the eigen-phase displacement over all mesoscopic particles equals the integration over all field sources:

$$r = \int \prod r(y) dy^3 = \prod \int r(y) dy^3 = 2\epsilon_0 \prod r_s(x) / 2\epsilon_0 \quad (20)$$

Performing a Fourier transform on the eigen-phase displacement heterogeneity $a(t)$ yields:

$$a(q) = \sum_i a(x_i) e^{-iqx_i} \approx iq \sin(2\epsilon_0 q) a \approx iq^2 \ln r \quad (21)$$

We now articulate the fundamental distinction between thermodynamic inertia and Newtonian inertia from the perspective of algebraic group structures. For a non-equilibrium system under “thermodynamic infinite”, the collective state of all Mean Areas (MAs) and their correlations can be described at any given instant. Under the definition of the MA, each such region or correlated set is characterized by a vector formed from its degree of non-equilibrium and its relative volume($v(x)=V(x)/dV$), denoted as $(r(x), v(x))$. The set of all such vectors, combined with a specific multiplication rule that represents the aggregation of their non-equilibrium degrees, forms a **semi-group**. Here, x is a spatial coordinate, $r(x)$ is the eigen-phase displacement of MA(or a correlated set of MAs) at x . $V(x)$ is the volume of that MA at x , dV is the volume of a minimal, fundamental MA. The parameter $v(x)=V(x)/dV$ is thus the relative volume ratio.

The multiplication operation for this semi-group is defined as follows:

$$(r_s(x), v(x)) * (r_s(y), v(y)) = (r_s(xy), v(x)+v(y)) \quad (22)$$

$$r_s(xy) = e^{\frac{(\Delta E(x)v(x) + \Delta E(y)v(y))}{(v(x)+v(y))kT}} \quad (23)$$

Equation (23) holds for subsystems of any size, as it is a direct corollary of Equation (16). The demonstration of the semi-group is:

1. Closure

Based on the assumption of spatial infinity and the MSS cutting theorem, any individual mesoscopic MA or collective of multiple MAs within the scope of the cutting set can, in principle, occur. A valid MA need only satisfy the following condition:

$$\Delta E(z) \in [(\Delta E(\min), (\Delta E(\max))]$$

If $(r_s(x), v(x))$ and $(r_s(y), v(y))$ are two elements within the set, then according to the multiplication rule:

$$(r_s(x), v(x)) * (r_s(y), v(y)) = (r_s(xy), v(x)+v(y))$$

$$\Delta E(xy) = \frac{(\Delta E(x)v(x) + \Delta E(y)v(y))}{(v(x)+v(y))} \in [(\Delta E(x), (\Delta E(y))]$$

There must exist a state z such that $\Delta E(z) = \Delta E(xy)$. This guarantees that $(r(z), v(z))$ is a member of the set, thereby proving closure.

2. Commutativity

$$((r_s(x),v(x))*(r_s(y),v(y)))*(r_s(z),v(z)) = (r_s(xyz),v(x)+v(y)+v(z)) = (r_s(x),v(x)) * ((r_s(y),v(y)) * (r_s(z),v(z)))$$

So, this operation satisfies closure, associativity, and commutativity. The set of all such vectors therefore constitutes a commutative semi-group (which becomes a monoid if the formal identity element $(1, 0)$ is included). Crucially, this semi-group lacks inverse elements.

This algebraic structure directly embodies the irreversibility of time's arrow, which is the fundamental distinction between thermodynamic inertia and classical Newtonian inertia. Newtonian inertia originates from the conservation of momentum; its superposition obeys vector addition, corresponding to a Lie group structure (e.g., translation or rotation groups), which possesses complete inverse elements (reversed velocity or momentum). In contrast, thermodynamic inertia arises from the directed drive of time's arrow; its superposition obeys the defined multiplication, corresponding to a semi-group structure. The former describes reversible mechanical motion, while the latter describes irreversible thermodynamic relaxation. The distinctions between the two are summarized in the table 1 below.

Properties	Newton inertia	Thermodynamic inertia
Mathematical structure	Lie group	Semi-group
Combination Rule	Vector Addition	Special multiplication
Effective scale	Upon quantum scale	Mesoscopic scale
Originating Principle	Conservation of momentum	Arrow of time

Table 1, the difference of Newton inertia and thermodynamic inertia

The eigen-phase displacement described by Equation (12) and (14) are useful but complicated. To address the exact relationship of r and ω , we consider the thermodynamic probability of an arbitrary microstate within the system, denoted as $f(i_p, N) = P(i)$, where i_p is the number of particles in a non-equilibrium state and N is the total number of particles, i is the microstate sequence index. For a given “equilibrium” local region in the non-equilibrium system, if we neglect the impact of dynamical heterogeneity on boundary conditions, the partition function can be expressed as:

$$Z_{\text{equilibrium}} = \sum_i^W P(i) = \sum_{ip=0}^N f(i_p, N) \quad (24)$$

If we “drive” this “equilibrium” local into a non-equilibrium local, then:

$$Z_{\text{Non-equilibrium}} = \sum_i^{W/\omega} P(i) = \frac{\sum_{ip=0}^N f(i_p * r, N)}{\omega r} \quad (25)$$

Thus, there exists an identity:

$$\lim_{N \rightarrow \infty} \frac{\sum_{ip=0}^N f(i_p, N)}{\omega r} - \sum_{ip=0}^N f(i_p * r, N) = 0 \quad (26)$$

Therefore, the critical parameters for the non-equilibrium transition can be determined by calculating the r parameter.

$$\omega r = \frac{Z_{eq}}{Z_{ne}} \quad (27)$$

As defined in Equation (14) and (17), the parameter $r(x+\epsilon), r_s(x), r$ could be treated as a correction to the thermodynamic probability for each mesoscopic particle, MA and total system. It is related to the collective effect of dynamics of every individual particles, thus having broader research significance.

Note that substituting equation (14) into equation (2) yields a key equation governing the non-equilibrium phase transition.

$$E - ST - T \int_t^{t+\Delta t} J dt \geq N k T \ln r \quad (28)$$

It determines whether the non-equilibrium phase can still be maintained along its current relaxation path. While Prigogine's theory of open systems addressed how systems and their environment construct a "non-equilibrium balance", the concepts of thermodynamic inertia and eigen-phase displacement explains why, within the system itself, each subsystem and even each particle tends to reside in a non-equilibrium phase beyond equilibrium, and why transitions in non-equilibrium relaxation pathways occur. The new theoretical framework aligns with Prigogine's thinking within the thermodynamic theoretical system, representing an inevitable consequence of the continuous driving by the second law of thermodynamics. Relevant data and experimental validation will be presented in subsequent sections. Next, let's put the eigen-phase displacement into the **mesoscopic** Liouville equation to build the new MCT function.

1.3 the second part of eigen-phase displacement theory: MCT

First, we consider the vector A composed of density modes and currents in wave-vector space:

$$A = \begin{bmatrix} \delta \rho_q \\ J_q^L \end{bmatrix} = \begin{bmatrix} \sum_i e^{i\vec{q} \cdot \vec{x}_i} - (2\pi)^3 \rho \delta(\vec{q}) \\ \frac{1}{m} \sum_i (\vec{q} \cdot \vec{p}_i) e^{i\vec{q} \cdot \vec{x}_i} \end{bmatrix} \quad (29)$$

Next, we present the ensemble-averaged correlation expression for vector A in non-equilibrium phase space:

$$C_{ne}(t) = \langle A^*(0) A(t) \rangle_{ne} = \sum_{j=1}^{W/\omega} A^*(0) A(t) e^{-E_j/k_B T} / Z_{\text{Non-equilibrium}} \quad (30)$$

For mesoscopic particles, considering that the eigen-phase displacement constitutes an obligatory expenditure of free energy, that is to say, the Hamiltonian must encompass the energy associated with eigen-phase displacement. Consequently, the Liouville equation can be expressed as:

$$\frac{dC}{dt} = \{C, H(\omega)\} = \{C, H_0\} + \{C, \Delta E(x)\} \quad (31)$$

$$= iLC + \{C, k_B T \ln r(x)\} = iLC - k_B T \sum_{i,j \neq i} \frac{\partial \ln r(ij)}{\partial \vec{x}_i} \frac{\partial}{\partial \vec{p}_j} C = iLC - \Xi \quad (32)$$

The potential field of thermodynamic inertia force is formed in space by the gradient of eigen-phase displacement $\frac{\partial \ln r(ij)}{\partial \vec{x}_i}$. The direction of the gradient is pushing the particle back to the eigen-phase. When coupled with density fluctuation modes, this collective effect manifests as a multiplicative enhancement of the restoring force term, which scales linearly with the eigen-phase displacement heterogeneity $a(t)$. Physically, this implies that stronger non-equilibrium heterogeneity leads to a more pronounced confinement effect on density fluctuations. Note that

this new interaction term, originating from the eigen-phase displacement, can be simplified as:(details could be seen in SI B)

$$\Xi = \left[\begin{array}{c} 0 \\ -\frac{iqNk_B Ta(q)}{m} F(q,t) - q^2 \sum_j^m \vec{p}_j e^{-i\vec{q} \cdot (\vec{x}_j - \vec{x}_j(t))} \end{array} \right] \quad (33)$$

$$a(q) = \sum_i \sum_{j \neq i} \frac{\partial \ln r(ij)}{\partial \vec{x}_i} e^{-iqx_i} = iq \int \ln r(x) e^{-iqx} d^3x \approx iaq^2 = iq^2 \ln r \quad (34)$$

The new term Ξ originates from the gradient of the thermodynamic inertial potential $k_B T \ln r(x)$. Its net effect is equivalent to introducing, at each spatial point, an additional restoring force field proportional to the local gradient of the eigen-phase displacement. We note that since the thermodynamic inertia force stems from the arrow of time, and time itself is homogeneous in space, its Fourier-space representation, $a(q)$, must exhibit even symmetry. The functional form of the thermodynamic inertial potential is elaborated in SI B.

For a given non-equilibrium system, the equation (32) could be simplified by the Mori-Zwanzig projection operator(details can be seen in SI B):

$$\frac{d^2 F_{ne}(q,t)}{dt^2} + q^2 k_B T / m \left(\frac{1}{S_f(q)} + aq^2 \right) F_{ne}(q,t) + \frac{m}{Nk_B T} \int_0^t \langle R_{-q} R_q(\tau) \rangle \frac{dF_{ne}(q,t-\tau)}{d\tau} d\tau = 0 \quad (35)$$

If $a = 0$, which corresponds to zero heterogeneity in the degree of non-equilibrium and is physically equivalent to a zero degree of non-equilibrium, the equation (35) reduces to the MCT equations for equilibrium systems, i.e., the standard NMCT equations:

$$\frac{d^2 F_{eq}(q,t)}{dt^2} + \frac{q^2 k_B T}{m S_f(q)} F_{eq}(q,t) + \frac{m}{Nk_B T} \int_0^t \langle R_{-q} R_q(\tau) \rangle \frac{dF_{eq}(q,t-\tau)}{d\tau} d\tau = 0 \quad (36)$$

1.4 The MSS-MCT equation

For any system subsystem, and each mean area, we get the combination of equation (28) and equation (36) to be the MSS-MCT equation:

$$\left\{ \begin{array}{l} E - ST - T \int_t^{t+\Delta t} J dt \geq Nk_B T \ln r(MSS) \\ \frac{d^2 F_{ne}(q,t)}{dt^2} + q^2 k_B T / m \left(\frac{1}{S_f(q)} + aq^2 \right) F_{ne}(q,t) + \frac{m}{Nk_B T} \int_0^t \langle R_{-q} R_q(\tau) \rangle \frac{dF_{ne}(q,t-\tau)}{d\tau} d\tau = 0 (MCT) \end{array} \right. \quad (37)$$

This system of equations explains many issues, with the most interesting aspect being the correlation between $Nk_B T \ln r$ and $q^2 k_B T / maq F_{ne}(q,t)$. Firstly, these two terms illustrate that the arrow of time, as a fundamental principle, can be embodied in both equations simultaneously, which is a profound natural attribute of physical laws. Secondly, the critical point of non-equilibrium phase transitions is constrained by $Nk_B T \ln r$, while the cage-effect is significantly enhanced by $q^2 k_B T / maq F_{ne}(q,t)$. Finally, it must be added that this system of equations holds not only for the non-equilibrium system as a whole, but also for each MA.

For nearly isolated systems (e.g., glass formers), the $J \approx 0$, so we get:

$$\left\{ \begin{array}{l} E - ST \geq Nk_B T \ln r \\ \frac{d^2 F_{ne}(q,t)}{dt^2} + q^2 k_B T / m \left(\frac{1}{S_f(q)} + aq^2 \right) F_{ne}(q,t) + \frac{m}{Nk_B T} \int_0^t \langle R_{-q} R_q(\tau) \rangle \frac{dF_{ne}(q,t-\tau)}{d\tau} d\tau = 0 \end{array} \right. \quad (38)$$

Equation (38) holds only for non-equilibrium systems that conform to the assumptions of

$J \approx 0$, and it is simpler for non-living systems. Furthermore, because this force acts on mesoscopic particles, any subsystem with a characteristic size below a certain cutoff scale should be considered in a state of equilibrium or near-equilibrium, effectively recovering the local equilibrium assumption. In Fourier space, this corresponds to the existence of an upper cutoff in the wavenumber q . This cutoff naturally emerges within the MSS-MCT equations, though a detailed discussion is beyond the scope of the main text and can be found in SI B. Now, let's see what's the new results reasoned from this new theory, especially the dynamics and thermodynamics.

II. Dynamical Theoretical verification: Non-Gaussian Parameters

Solving Equation (38) is largely analogous to solving a Newtonian mechanical equation; it necessitates introducing appropriate approximations to simplify the memory kernel $\langle R_{-q} R_q(\tau) \rangle$. Different approaches, such as NMCT (Standard Mode-Coupling Theory)²⁶, GMCT (Generalized Mode-Coupling Theory)⁵⁵, EMCT (Extended Mode-Coupling Theory)⁵⁶, Elastic Theory of the Glass Transition⁵⁷, and NLE (Nonlinear Langevin Equation) theory⁵⁸, provide distinct pathways for this simplification.

In principle, methods like GMCT and EMCT offer more sophisticated treatments of the memory kernel. However, for addressing the core issue of thermodynamic inertia, employing different simplification schemes does not alter its fundamental nature. Therefore, to most clearly highlight the critical role of the a term, this paper employs the simplest NMCT approximation. The detailed solution can be found in SI B and SI C:

$$F_{ne}(q,t) = \frac{S_f(q)}{2} - S_f(q) c_0 t \sqrt{1 - 4(1 + aq^2 S_f(q)) / \lambda}, \tau \gg 1 \quad (39)$$

Here, t denotes time, c_0 is a numerical parameter, and λ is the “controll parameter”.

It is important to note that the true glass transition critical point predicted by MSS-MCT is determined by the MSS equation. At this critical point, the free energy is entirely converted into eigen-phase displacement, leading to a minimization of purely dissipative fluctuations. Consequently, the predicted glass transition temperature is significantly lower than that forecasted by standard NMCT. This aspect will be discussed in the next chapter. Note that the solution given by Equation (39) represents how $F(q,t)$ approaches a plateau. The evolution of $F(q,t)$ is further constrained by the MSS equation in equation (38). If the temperature is held constant, the MSS-MCT theory predicts the following scenario for the intermediate scattering function: it first decays to a plateau region, then remains nearly constant on this plateau until the available free energy sustaining the current non-equilibrium state is exhausted, after which it transitions to a new plateau.

In addition to eigen-phase displacement, several important parameters have been proposed to characterize the degree of non-equilibrium, such as the T-M measure and the non-Gaussian parameter. This paper focuses specifically on theoretical results for the non-Gaussian parameter, which can be directly derived from the Taylor expansion of $F(q, t)$:

$$F(q,t) = 1 + \frac{1}{2!} \langle q^2 \Delta r^2 \rangle + \frac{1}{4!} \langle q^4 \Delta r^4 \rangle + \dots \quad (40)$$

Furthermore, Equation (38) demonstrates that $F(q, t)$ is influenced by a strong generalized force, making it more difficult for particles to escape their cages. This will lead to greater deviations in both $\langle \Delta r^2 \rangle$ and $\langle \Delta r^4 \rangle$. What is more intriguing is that structural heterogeneity and

heterogeneity in the degree of non-equilibrium become coupled. It is precisely this coupling between inertias of distinct algebraic origins (semi-group vs. group) that leads to a significant amplification of the cage effect, which manifests dynamically as a large non-Gaussian parameter α_2 . Let us briefly elucidate the origin of this coupling phenomenon.

Starting from Equation (38) and applying the transformations $F_{ne}(q,t)=\Phi(q,t)S(q)$ and $L\{\Phi(q,t)\}=\Phi(q,z)=\int_{-\infty}^{+\infty}\Phi(q,t)e^{-izt}dt$, we get:

$$\frac{\Phi(z)}{1+iz\Phi(z)}=\frac{1}{(1+aq^2S_f(q))\Omega^2}(-iz+\Omega^2\lambda\int_0^{\infty}\Phi(t)^2e^{izt}dt) \quad (41)$$

Note that, regardless of the values of time t , frequency z , or wavevector q , the left-hand side of the equation must retain a dependence on q . This is due to the presence of an irreducible term on the right-hand side, $(1+aq^2S_f(q))$. The origin of this term lies in the fact that the eigen-phase displacement heterogeneity $a(t)$ does not conform to the multiplicative rules governing the gradient of Newtonian inertia. Consequently, these two distinct types of inertia can only couple in the form shown, and cannot be unified into a single term like $kS_f(q)$.

Considering that the critical point constrained by the MSS equation is in fact located relatively far from the plateau region (a detailed analysis can be found in the next chapter), the final expression for the non-Gaussian parameter is derived as follows(details could be seen in SI C):

$$\alpha_2(\text{peak-}ne)=\lim_{q\rightarrow 0}\frac{2\left[\left(\frac{1}{2}-K\right)S_4+K\gamma S_0S_2+\frac{K\gamma^2S_0^3}{8}\right]}{\left[\left(\frac{1}{2}-K\right)S_2+\frac{K\gamma S_0^2}{2}\right]^2}-1 \quad (42)$$

In equation (42), $S_0=S_f(0), S_2=\frac{1}{2}S_f''(0), K=c_0\tau\sqrt{1-\frac{4}{\lambda}}, \gamma=\frac{4a}{\lambda-4}, \tau$ is the dynamic transition time.

If $a=0, r=1$, then the peak of NGP of MSS-MCT would return to the NGP of NMCT:

$$\alpha_2(\text{peak-}eq)=\lim_{q\rightarrow 0}\frac{2S_4}{\left(\frac{1}{2}-K\right)S_2^2}-1\approx 0.1 \quad (43)$$

Comparing the NGP of MSS-MCT and NMCT in the following equation:

$$\alpha_2(\text{peak-}ne)\approx\lim_{q\rightarrow 0}\frac{2\left[K\gamma S_0S_2+\frac{K\gamma^2S_0^3}{8}\right]}{\left[\left(\frac{1}{2}-K\right)S_2+\frac{K\gamma S_0^2}{2}\right]^2}+\alpha_2(\text{peak-}eq) \quad (44)$$

This expression reveals a universal positive correlation between the non-Gaussian parameter α_2 and the plateau value of the intermediate scattering function, $F_{ne}(0,\tau)$. By using neutron scattering⁵⁹, SPT⁶⁰, DDM⁶¹ and computer simulations, this quantitative relationship aligns, both qualitatively and quantitatively, with experimental observations across various glass-forming systems such as small particles⁶², colloids^{63,64} and polymers^{65,66}.

By inputting the structure factor $S_f(q)$, the plateau value of the intermediate scattering function $F(q,\tau)$, and the eigen-phase displacement heterogeneity a into the equation(36), one obtains the theoretical value of the non-Gaussian parameter α_2 predicted by the MSS-MCT theory. It is important to note that while both $S_f(q)$ and the plateau value of $F(q,\tau)$ can be taken from experimental or simulation data, the required precision is exceptionally high, particularly for the

second derivative of the structure factor. Furthermore, the parameter a must be obtained by solving the MSS equations. In the next chapter, where we solve the MSS equations for the polymer model, we find $a \approx 0.04$. This parameter is deeply connected to the spatial configuration of the system; therefore, its value may vary in other material systems. Nevertheless, it remains valuable for a preliminary analysis of the non-Gaussian parameter.

Due to the limited availability of publicly accessible, complete $S_f(q)$ datasets, the theoretical curves presented here demonstrate the predicted trend based on the typical range of values reported in the literature⁶²⁻⁶⁶. From these literature sources, it is evident that for colloidal glasses, small-molecule glasses, and polymer glasses alike, the values of both S_0 and S_2 are very small. S_0 typically falls within the range of approximately 0.01 to 0.1, while S_2 is even smaller, roughly between 0.001 and 0.01. Here, S_0 can be estimated from parameters such as the compressibility, number density, and glass transition temperature, whereas S_2 usually relies on precise simulation data, for instance, the Lennard-Jones particle data provided in Theory of Simple Liquids⁶⁷. To avoid introducing additional theoretical calculation errors, we directly substitute different sets of S_0 and S_2 data into the equation (44) for verification. The calculated results of α_2 for systems with different structure factors are presented in Figure 3. Variations of these parameters within a reasonable range will quantitatively affect, but not qualitatively alter the scaling relationship trend between α_2 and $F(q,\tau)$. This result verifies the robustness of the core mechanism of the MSS-MCT theory.

Crucially, our theory resolves the order-of-magnitude discrepancy in the non-Gaussian parameter: while standard NMCT yields 0.1, MSS-MCT correctly predicts α_2 falls within the range of 1 to 10, in quantitative agreement with experiments across diverse glass-forming systems. Overall, the peak value of α_2 shows a positive correlation with the intermediate function $K(\text{peak}) \propto \tau \propto 1/\langle \Delta x(t)^2 \rangle_{\text{ne}}$ and an inverse relationship with the mean-square displacement. This implies that when the cage is sufficiently tight, the relaxation time becomes long enough, consequently leading to a sufficiently high non-Gaussian parameter—a conclusion entirely consistent with the physical mechanism of the glass transition⁶⁸. This trend, however, is not absolute. Should the plateau value of $F(q,\tau)$ approach too close to 1, indicating a system nearing a random solid state or even a solid state, the non-Gaussian parameter would necessarily decrease—a scenario not encountered in the liquid-state systems studied here.

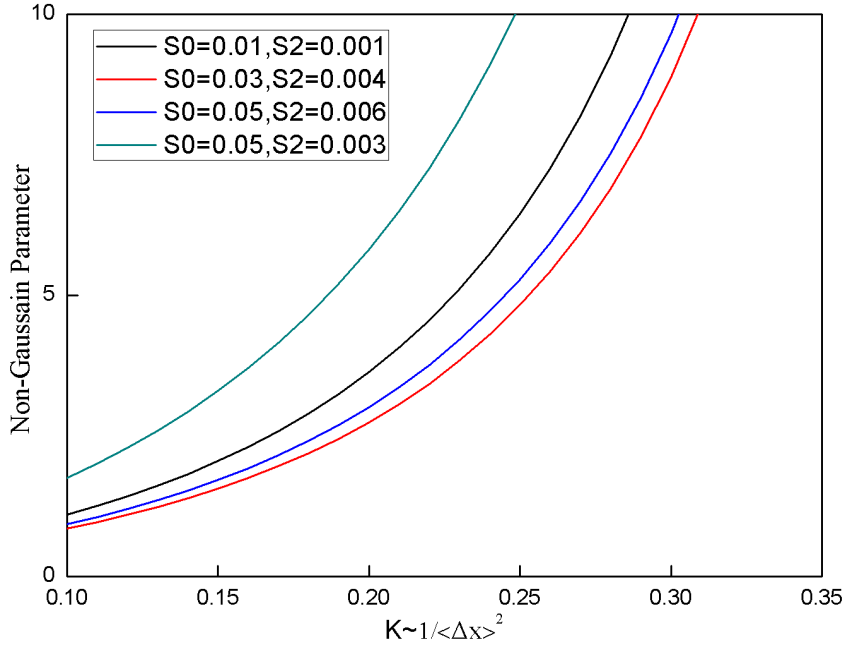


Figure 3. the relationship of NGP(peak) and $K(\text{peak})$ in MSS-MCT theory for systems with different structures. $K(\text{peak}) \propto \tau \propto 1/\langle \Delta x(t)^2 \rangle_{\text{ne}}$, So, NGP(peak) is inverse to mean square distance.

III. Thermodynamical Theoretical verification: C1 in polymers

3.1 The Thermodynamics and the “constant” C1 in Flory’s conjecture

According to the MSS equation, the critical point represents a boundary that is physically impassable. Let the critical point be denoted as t_c . For $t > t_c$, the path is a virtual (unphysical) trajectory. Therefore, along this virtual path, the entropy must necessarily diverge; that is:

$$E(t) - S(t)T \geq Nk_B T \ln r(t) \rightarrow \lim_{t \rightarrow t_c^+} \frac{\partial S(t)}{\partial t} = \infty \quad (45)$$

From Equation (45), we can get a constant to represent the critical point:

$$\text{Constant} = C(E - ST - T \int_t^{t+\Delta t} J dt - Nk_B T \ln r) = C(0) \quad (46)$$

If the degree of non-equilibrium is further increased, the system can only relax anew on a completely fresh reference sequence. The description of such new reference sequences requires the deep involvement of theories like replica theory, which falls beyond the scope of the present work. This paper validates the existence of this multi-stage phase transition solely by demonstrating the divergence of the virtual path and by calculating the non-Gaussian parameter and the C_1 parameter for the non-equilibrium liquid/rubber state—which uses the equilibrium phase as its reference—prior to the critical point. A schematic illustration for a non-equilibrium system undergoing cooling is shown in the figure below.

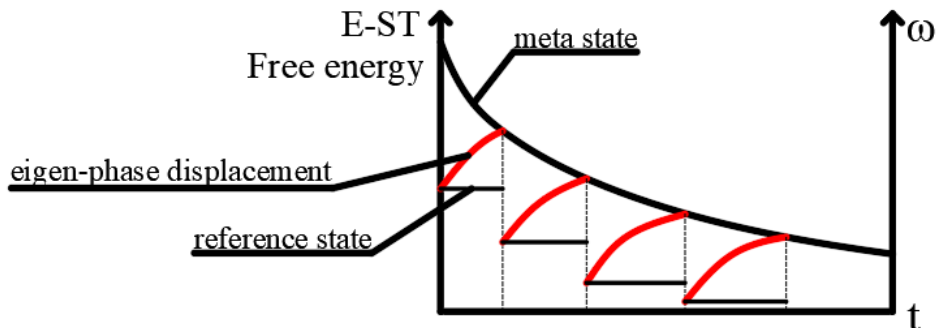


Figure 4. The scheme picture of free energy, non-equilibrium degree and time during a cooling process.

Figure 4 encompasses both the blue region (which is about to be proven) and the first prediction of this paper (to be discussed in the Discussion section, which states: "A non-equilibrium system approaching absolute zero, or a complex open system tending towards higher degrees of order, will undergo a process of repeatedly reaching the limit of its non-equilibrium degree, switching relaxation pathways, and then restarting the journey towards a new limit."). Figure 4, along with Equations (45) and (46), compels us to consider the following question: could the parameter from Flory's conjecture, C_1 , be precisely such a critically defined parameter that is rigorously determined by dynamics?

As the present work lacks methodologies from energy landscape theory, the Adam-Gibbs theory, replica theory, etc., which are required to analytically describe more advanced reference phases, we cannot directly derive the VFT or WLF equations from the MSS-MCT equations. Equation (38), however, indicates that only one parameter can be strictly defined as a universal constant. Consequently, the parameter C_2 in the WLF equation, which is often empirically found to be non-universal, must fall outside this category. Instead, it is one of the variable parameters linked to other core properties, such as fragility and relaxation time. This leaves C_1 as the sole candidate. The critical question then follows: is it indeed the universal constant?

It should be noted that our approach does not rely on the ill-defined notion of free volume. Nevertheless, a description entirely disregarding volume changes is insufficient to resolve C_1 , as the change in macroscopic volume remains the most prominent experimental signature of the polymer glass transition. To ensure the robustness of our analysis, we employ two complementary strategies. First, on a conceptual level, we describe the polymer volume strictly using two well-defined physical entities: voids (unoccupied lattice sites) and chain segments. This formulation deliberately and completely excludes the ambiguity inherent in the "free volume" concept. Second, on a theoretical level, we subject the entropy function of the polymer model to a rigorous robustness test around its critical point. This analysis provides definitive proof that the parameter emerging from this singularity is indeed Flory's universal constant C_1 .

3.2 First step: Projection of Polymer Ising model

Although linear polymer is natural one-dimensional material, the system still cannot be conveniently transformed into an Ising model in the same way as the lattice gas model. It requires a projection technique to simplify the polymer lattice model into a tractable Ising model form with intrinsic constraints:

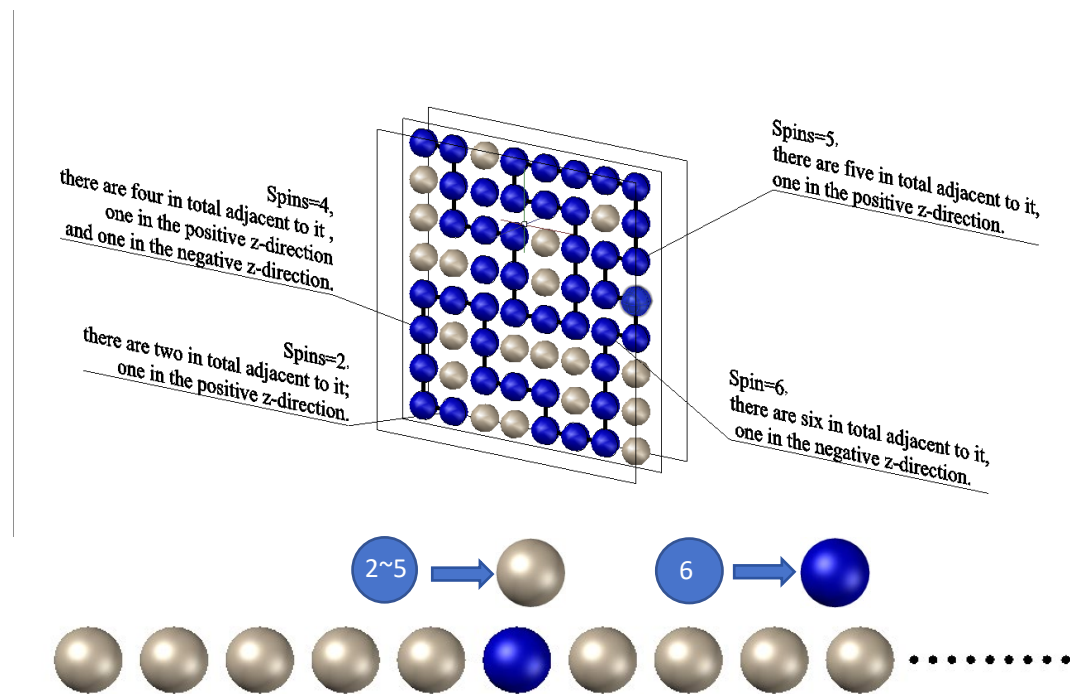


Figure 5. Schematic diagram of the simplified simple cubic lattice model for the polymer.

In the three-dimensional lattice, for a polymer chain, each monomer occupies a lattice site coordinated with six nearest neighbors. The coordination number of a site, that is, the number of adjacent lattice sites occupied by chain segments, is defined as its spin value. For example, in the topmost figure, the first site has a spin value of 4: it has two neighboring chain segments within the XOY plane, and one neighbor in each of the two adjacent planes perpendicular to it; in the middle figure, a projection is performed: sites with spin values between 2 and 5 are represented as white spheres, while sites with a spin value of 6 are projected as blue spheres. Sites with a spin value of 1 are omitted due to their negligible population; in the bottom figure, the white and blue spheres are connected according to their sequence along the polymer chain, forming a new "Ising chain" representing the instantaneous microstate of the system. All such microstates constitute the Microstate Sequence Space (MSS) for the polymer Ising model, indexed by the proportion of blue spheres. Within this MSS, the polymer chain always maintains a random coil conformation, exhibiting theoretical assumption of no structural symmetry breaking.

From Fig 5, we can see that the blue sites represent segments, and the white sites represent vacancies. Then we assign a number to each segment to record the total number of nearest neighbor and write the number in the center of blue ones. And finally, we treat spins with a value of 6 as new black spin in Ising chain, and spins that can take values between 2 and 5 as new white spin. We select the number of spins with a value of 6 as the order parameter in the MSS framework. This choice implies that the polymer chains remain random coils with invariant mean-square end-to-end distances throughout our derivation. Experimentally, neutron scattering studies have confirmed the constancy of the mean-square end-to-end distance during the glass transition^{69,70}.

We now employ the eigen-phase displacement to simplify the derivation by decomposing the six possible spin values into a more tractable form. For a "segment in equilibrium," it should be able to assume any spin value between 1 and 6. In contrast, for a segment in a non-equilibrium state, it can be approximated as being unable to access spin value 6. Thus, we write:

$$r_1 = \frac{P_{1-5}}{P_{1-6}} = 1 - \frac{P_6}{P_{2-5} + P_6} \quad (47)$$

We next consider a second decomposition scheme, in which all segments are divided into those that can assume spin values between 2 and 5, and those restricted exclusively to spin value 6. Clearly, near the glass transition critical point, the population of segments with spin value 6 becomes dominant. This makes the second decomposition more effective. Its relation to the first decomposition is given by:

$$\begin{aligned} r = r_2 &= \frac{P_6}{P_{2-5}} \approx \frac{P_{\text{(choosing to be segment in non-equilibrium)}}}{P_{\text{(choosing to be segment in equilibrium)}}} \\ &= \frac{P_{\text{(choosing to be segment in non-equilibrium)}}}{P_{\text{(choosing to be void in equilibrium)}}} \approx \frac{P_{\text{(choosing to be segment in non-equilibrium)}}}{P_{\text{(choosing to be void in non-equilibrium)}}} \\ &= \frac{1}{1-r_1} = 1 + \frac{1}{r_2} \end{aligned} \quad (48)$$

We proceed to derive the form of the entropy function using the eigen-phase displacement obtained from the second decomposition scheme. This approach leaves the physical meaning of the eigen-phase displacement unchanged; it merely simplifies the thermodynamic probability function through a straightforward mathematical transformation.

3.3 Entropy function analyze and picture of transition

Using equation (41) and MSS theory, we can get the r parameter to build the entropy function of linear polymer. The detailed deduction is written in SI D. And the final expression of entropy is:

Semi-Most-Probable Approximation: Only the probability distribution parameter r is retained to account for the role of MSS, while all microstates are treated as energetically equivalent.⁷¹ S is the entropy, N is the number of all sites, L is the number of segments in a single chain, G is the number of chains, r parameter is the eigen-phase displacement.

$$S = -\frac{k}{r} \ln \frac{N!}{(N-GLr)!} + kG(L-1) \ln \left(\frac{5}{N} \right) \quad (49)$$

Semi-Saddle-Point Approximation: The full details of the energy ordering are preserved, but the partition function is treated within a semi-saddle-point approximation. This is equivalent to multiplying the probability P by a factor $\frac{Z_{ne}}{c_n^{\rho}}$ (n is the total number of segment spins, ρ represents the number of spins with a value of 6).

$$S \approx Q \frac{(GL-r)!r!}{(GLr)!(\frac{GL}{N}(N-GLr))!} \quad (50)$$

Q is a non-divergent parameter whose expression is rather complex; its rigorous form is provided in SI D. These distinct approximation schemes demonstrate the **robustness** of the critical equation:

$$\left. \frac{\partial S}{\partial r} \right|_{N-GLr=0} = \infty \quad (51)$$

The two approximation schemes differ significantly in their mathematical and physical foundations—for instance, they yield substantially different expressions for the entropy function. However, the predicted critical point remains unaffected, thereby demonstrating the robustness of the conclusion. See Table 2.

Robust	Assumption	Error bar of Probability	The key equation
Semi-Most-Probable Approximation	The eigen-phase displacements of all MA are assumed to be equal	$Z_{ne} = \sum_{i=1}^{W/\omega} e^{-E_i/kT} \approx k \ln W^{1/r}$	$N-GLr=0$
Semi-Saddle-Point Approximation	The partition function of each MA only held the collection at Saddle-point.	$Z_{ne} = \sum_{i=1}^{W/\omega} e^{-E_i/kT} \approx C_N^{N-\rho r} e^{-E_{\rho}/kT}$	$\frac{GL}{N}(N-GLr)=0$

Table 2, Robust certification of entropy “virtual-divergence” at transition point

Equation (51) indicates the existence of a second-order phase transition point. The variation of entropy describes that if the system maintains the same relaxation behavior before and after the critical point, that is, if the form of the non-equilibrium variational function remains unchanged, the partial derivative will diverge and cause non-physics. Therefore, the system will inevitably experience a relaxation path at this critical point. In addition, the function describing the degree of non-equilibrium at this time is $N-GLr$. Based on the physical meanings of each parameter, it can be inferred that this function expresses whether the system has enough “volume” to accommodate the “ $N+l$ ”th Spin, or in other words, whether the system’s free energy at this time is sufficient to continue maintaining the MSS unchanged. Therefore, the definition equations (5) and (9) of the parameter r can be substituted into the function to obtain:

$$F-f(\omega)T \sim N-GLr \quad (52)$$

Equation (52) indicates that the displacement of eigen-phase has come to its limit at the glass transition critical point just as the degree of non-equilibrium. From equation (50), (51) and (52), the glass transition of linear polymer could be shown in fig 4.

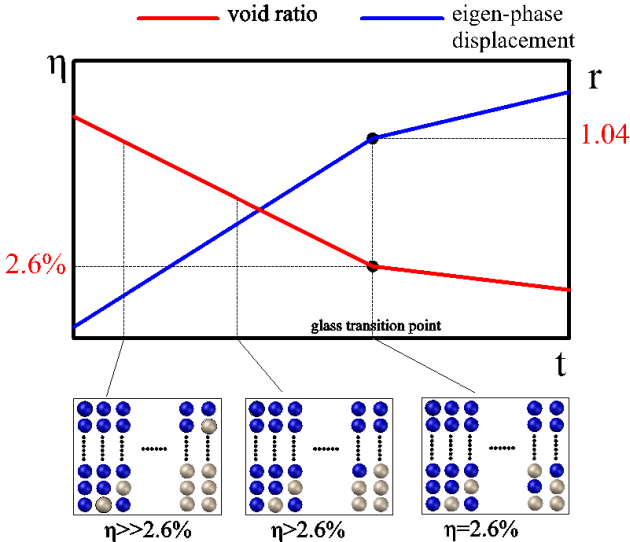


Figure 6. Evolution of eigen-phase displacement and vacancy fraction before and after the glass transition. The bottom axis represents time. The left axis represents the vacancy fraction. The right axis represents the eigen-phase displacement. The red line shows the variation in vacancy fraction across the glass transition. The blue line shows the variation in eigen-phase displacement across the glass transition. The inflection points in the red and blue lines correspond to the values attained when the system reaches the equilibrium state. The lower panel illustrates the evolution of the microstructural sequence in the non-equilibrium system before and after the glass transition and its relationship to the vacancy relative to the equilibrium state.

As shown in fig 6, only the void percentage of the critical point is certain, because it represents the limit of degree of non-equilibrium. All the uncertainty of degree of non-equilibrium would fall into certain at that point. The critical point vividly explains the relaxation process changes when the displacement of eigen-phase grows to its limit: If we ignore the power of the displacement of eigen-phase, which means $r \equiv 1$, then the entropy would never diverges as NMCT predicted. Now, let's solve the C_1 :

3.4 C1 of polymer

The critical equation is:

$$N-GLr=0 \quad (53)$$

By employing mathematical methods to eliminate the effect of chain ends on the entropy, we can modify the critical equation as follows:

$$N-GLr=0 \rightarrow 1 - \frac{r(\rho - \frac{2(\rho-1)}{6})}{N - \frac{2(\rho-1)}{6}} = 0 \rightarrow \frac{3}{1-\eta} = 2r(\omega) + 1 \quad (54)$$

$$\eta = \frac{V_{vacancy}}{V_{total}} = \frac{N-GL}{N} \approx \frac{n-\rho(\omega)}{n} \quad (55)$$

η is the void fraction (Since ϕ has already been used to denote the solution of the MCT equations in the preceding text, to prevent confusion, we will not use ϕ to label the volume). Thus, we obtain a function that depends only on the degree of non-equilibrium ω and temperature:

$$\frac{3n}{\rho(\omega)} = 2e^{\frac{\Delta E(\omega)}{kT}} + 1 \quad (56)$$

Equation (56) is overly complex. Nevertheless, it is indeed fully solvable. By fitting the curves describing the relationships between density, volume, and the degree of supercooling, one can solve for the parameter r , thereby rigorously proving that the value of the C_1 parameter is indeed a constant.

However, we can also analyze it more conveniently via Equation (54) based on a total volume

expansion hypothesis derived from extrapolating thermal expansion experiments. (It must be reiterated that this hypothesis does not involve the concept of free volume expansion. It does not require combining thermal expansion equations from two different system states to define that ill-defined "free volume"!) Since Equations (54) and (56) are equivalent, the resulting C_1 value obtained under this valid hypothesis will be the same.

Homogeneous volumetric expansion Hypothesis for single-phase systems: If the reference phase remains unchanged and the external pressure is constant, then the total volume is proportional to the temperature.

$$dV \propto dT \quad (57)$$

Note that this hypothesis **does not** suffer from the conceptual flaws associated with "free volume"; it is a strict extrapolation of experimental laws. Under this hypothesis, the total volume effectively becomes a function of the eigen-phase displacement:

$$\begin{aligned} & \left. \begin{aligned} & N \cdot GLr = 0 \\ & V = NdV \end{aligned} \right\} \rightarrow \eta = (N \cdot GL) dV = \eta(r) \\ & dV \propto dT \end{aligned} \quad (58)$$

From WLF equation³³, the relationship of C_1 and vacancy percentage is simple:

$$C_1 = \ln 10 / \eta(r) \quad (59)$$

Let it be reiterated that the "void" referred to here is **not** "free volume"; it is the vacancy volume under the volume expansion hypothesis. According to Equation (58), the core parameter C_1 is a transition factor strictly defined by the eigen-phase displacement. There is no recourse here to dynamics based on the notion that "particles require free volume to move." The dynamics corresponding to Equation (58) are instead governed by the strict cage-effect described by Equation (38), where relaxation motion and the eigen-phase displacement jointly determine the dynamics. The rigorous calculation process is provided in **SI E**, with the final result expressed as:

$$\eta = \frac{-19+3\sqrt{42}}{17} \approx 2.6\% \quad (60)$$

Converted to the C_1 parameter, it is $1/2.303 \cdot 2.6\% = 16.7$, let's compare it with experiments and classical theories.

From 1955, countless experiments have proved the correctness of C_1 by using DSC⁷², DMA⁷³, PAT⁷⁴ and et al⁷⁵. However, the non-fitting theoretical results is very few. So, we do not need to do more experiments to prove the C_1 , but we should compare our theoretical result with the experiments and classical theories in the Table 3.

Theory	Vacancy(%)	C_1	Error vs Experiments	Hindered physics
Simha-Boyer (1962)	11.6%	3.7	455%	Vibration volume
Cohen-Grest (1979)	7.6%	5.7	300%	L-J potential
Adam-Gibbs (1965)	5.3%	8.2	207%	CRSS
MSS result (Our work)	2.6%	16.7	1%	Eigen-phase displacement

Table 3. Theoretical and experimental values of C_1

From Table 3, our theory has the best accuracy to prove itself. The physical picture behind the 2.6% is the limit of displacement of eigen-phase. In another explanation, the transition

happens on the critical point that the free energy of the non-equilibrium system were just enough to pay the “cost” of self-driving relaxation. For linear polymers, the Positron Annihilation Lifetime Spectroscopy (PALS) measures the glass transition temperature (T_g) by detecting the critical point at which the relative void fraction reaches approximately 2.5~2.6%. The T_g values obtained via PALS are consistent, within experimental error, with those measured by Differential Scanning Calorimetry (DSC) and other techniques. This agreement confirms that the glass transition temperature predicted by the MSS-MCT theory aligns with the experimentally observed T_g within the margin of error.

It is noteworthy that the calculation of C_1 within the MSS-MCT theory is confined to linear polymers and is valid only under conditions where the negative entropy flux from the environment is negligible. For certain polymer systems of higher complexity or under different experimental conditions, the **random packing** assumption may provide a more suitable description than the homogeneous volumetric expansion hypothesis for single-phase systems adopted in this work, leading to **different results**⁷⁶. However, these outcomes do not violate the principles of mesoscopic dynamics or the second law of thermodynamics. Consequently, we conjecture that they do not contravene the MSS-MCT equations either, but merely necessitate more sophisticated treatment.

Lastly, this constant C_1 has three physical meanings: First, it represents the point at which the displacement of eigen-phase reaches its limit at a given temperature; second, it signifies the critical boundary between the rubbery (or liquid) state and the glassy state; and third, it figured out the nature of polymer glass transition. A simpler way to understand glass transition is to consider voids as the “solvent” and polymer chains as the “solute”. The critical point of the glass transition then represents the upper limit of the “supersaturation” of the polymer chains. If accuracy is everything, the Flory’s conjecture is resolved in this paper. Now, the thermodynamics of Polymer glass transition has been explained by thermodynamic inertia theory.

IV. Discussion and outlook

The thermodynamic inertia force proposed in this work, through the distinctive properties of its semi-group algebra, unifies the thermodynamic and dynamic descriptions of non-equilibrium systems. This is reflected in the following aspects: on the thermodynamic side, it determines the phase transition boundary (C_1) by constraining the free energy consumption (the MSS equation); on the dynamic side, it amplifies dynamic heterogeneity (α_2) by enhancing the restoring force term (the a term in the MCT equation). Both are connected through the same parameter of eigen-phase displacement r . Next, we will discuss its application to other challenging problems, its connections with other theories, and its theoretical predictions.

4.1 Interpretation of the Kauzmann Paradox

Let us now examine whether this theory can provide a reasonable explanation for the Kauzmann paradox. As can be seen from fig 4, at the critical point, the system can no longer evolve along its original relaxation path toward a more “ordered” non-equilibrium state. If the second law of thermodynamics and the environment drive it to continue evolving, its relaxation path must undergo a transition—meaning that the set of accessible microstates or its reference phase can no longer be the equilibrium phase. Therefore, building upon the MSS-MCT theory, we propose the following conjecture to try to explain the Kauzmann paradox:

After undergoing multiple or even innumerable non-equilibrium transitions, the reference

phase of a non-equilibrium system will progressively deviate further from equilibrium, until the number of microstates in the reference phase reaches a minimum. In other words, our theory predicts that the entropy-temperature curve of a non-equilibrium system cannot be extrapolated to a straight line. At the critical point where free energy is exhausted, the system will continuously contract its reference phase, leading to a different theoretical scenario depicted in coupling of Energy Landscape theories and MSS-MCT theory.

4.2 The lower temperature transitions and the importance of reference states

As previously established, for systems approaching the ideal glass transition, their reference phase is already far from equilibrium. It should be noted that this phenomenon is not necessarily confined to low temperatures; living systems serve as crucial evidence for the existence of such reference phases. Upon biological death, not all cells perish immediately; rather, specific tissues composed of these cells lose their function. For example, the human heart remains viable for several hours post-mortem⁷⁷, allowing for organ donation. However, the MSS-MCT equations do not provide a complete methodology for calculating such advanced reference phases. The reference phase used in this work is the most fundamental equilibrium phase, universally recognized.

Theories within the energy landscape framework represent the most robust and key methods for this purpose. This is because the concept of meta-states can bridge MSS theory and energy landscape theory, with the latter being the optimal methodology for describing meta-states—exemplified by the cooperatively rearranging regions (CRR) in the Adam-Gibbs theory. However, constrained by the breadth of the author's research focus, this paper will not extend the discussion further on this front.

4.3 Field theory and eigen-phase displacement

You may have noticed that the conceptual entities of the eigen-phase displacement in the MSS and MCT equations—that is, their operational definitions in a physico-philosophical sense—coincide only in the thermodynamic limit due to differences in continuity. Although this paper defines the eigen-phase displacement axiomatically from the arrow of time, at the level of operational definition, to achieve a complete description of real systems beyond the thermodynamic limit, the optimal approach would be to generalize the MSS-MCT equations starting from the field-theoretic formulation of mode-coupling theory developed by David Reichmann⁷⁸. As this paper aims to eliminate or minimize fitting parameters and attempts to preserve the flexibility of the MSS sequence representation, we have not undertaken this generalization of the MSS-MCT equations here. However, it is foreseeable that the generalized equations would find better application in other domains.

4.4 Why the MSS-MCT framework constitutes an intrinsic extension of Prigogine's theory

Prigogine's groundbreaking work established that open systems can maintain non-equilibrium steady states by importing negentropy from their environment. However, his phenomenological description left open a fundamental question: How does this imported negentropy translate, at the mesoscopic level, into a force that actively maintains a specific non-equilibrium configuration from **within**?

Our theory of eigen-phase displacement provides the missing link. We identify r as the internal conservative force that actively restores fluctuations back to the non-equilibrium eigen-phase. The generalized MSS criterion then explicitly couples this internal force to the external entropy flux:

$$E-ST-T \int_t^{t+\Delta t} J dt \geq Nk_B T \ln r$$

This equation reveals a profound duality:

In isolated/closed systems, the eigen-phase displacement is a transient inertial force fueled by internal free energy, explaining the stretched relaxation and eventual equilibrium in systems like glasses;

In open systems, a persistent negative entropy flux continuously replenishes the eigen-phase displacement, transforming it from a transient inertia into a sustained vital force. This is the thermodynamic essence of life and other dissipative structures.

Thus, our theory does not contradict Prigogine's; it completes it by providing the mesoscopic dynamical mechanism from **within** that underlies his phenomenology from the **outcome**. The eigen-phase displacement is the physical embodiment of the "organizing principle" that imported negentropy activates in living and driven matter.

4.5 Theoretical prediction

Based on our theoretical achievements, we propose the following predictions:

1. The semi-group structure of thermodynamic inertia implies that if a system never reaches equilibrium, its history of thermodynamic inertia does not vanish, as there exists no inverse element to cancel it. Consequently, we predict that in non-equilibrium systems such as glasses, even after prolonged annealing or physical aging, the 'thermodynamic inertia imprint' determined by their early formation history (e.g., cooling rate) will persist and continuously influence their nonlinear mechanical response and failure behavior. This stands in fundamental opposition to predictions based on equilibrium-state assumptions, which hold that historical effects can not be entirely erased.

2. Dendritic segregation in crystallizing systems also presents an excellent candidate for investigation within the MSS-MCT framework. Notably, significant dendritic segregation can be observed even under very small temperature gradients and very slow crystallization rates. Phenomenologically, this bears a striking resemblance to the mechanism in glass-forming systems, where the coupling between the thermodynamic inertia force and the structural inertia force gives rise to a dramatically enhanced non-Gaussian parameter. In this sense, the MSS-MCT theory provides a unified perspective for understanding how the thermodynamic inertia force, through its coupling with other inertia forces, can drive pronounced non-equilibrium phenomena across diverse material systems.

3. The eigen-phase displacement can couple with the entropy flux from the external environment. The thermodynamic inertia force would be proved to be the origin of entropic driving force. This signifies that by actively modulating external entropy flows (e.g., via optical, chemical, or mechanical driving), we can non-invasively 'program' the non-equilibrium states within matter—for instance, enhancing or suppressing its glass-forming tendency or altering its relaxation spectrum. This opens a new avenue for designing novel intelligent dissipative materials.

4. Life possesses an indisputable "agency." Even unconscious organisms can seek benefit and avoid harm, delay aging, and resist death. Merely obtaining the drive to maintain low entropy from external negentropy flows is only the surface of the "vital force" problem. Life can actively intake food that is not particularly low in entropy within a stable environment, yet create and expel

high-entropy waste to sustain itself. If necessary, organisms can even shed parts of their bodies to survive longer. Any viable concept of a vital force must effectively address these issues. We posit that the thermodynamic inertia force is likely the true source of the vital force, for three reasons: First, it can transform with entropy flow, serving as an internal thermodynamic driving force. Second, it is a sustaining force that maintains the current non-equilibrium state under any conditions. Finally, given specific initial conditions, it indeed drives the system to choose a "more favorable" direction rather than succumbing to death. Therefore, we propose this hypothesis to provide a clearer and more complete interpretation of the vital force.

This thermodynamic inertia, together with the MSS-MCT equations, will reshape the understanding of non-equilibrium thermodynamics, establishing the eigen-phase theory as a universal framework for studying complex systems, from glasses to living organisms.

V. Summary

In summary, this work operationalizes the arrow of time into a thermodynamic inertia force that acts on mesoscopic particles. This establishes the first first-principles mesoscopic framework—the Microstate-Sequence-Mode-Coupling (MSS-MCT) theory—that unifies the thermodynamic and dynamic descriptions of non-equilibrium matter. The body of evidence presented across different material systems and distinct physical puzzles demonstrates the correctness of the new theory. This theory identifies a “conservative” force, sustained against fluctuations, which obeys a semi-group algebra. This mathematical structure is fundamentally different from the Lie group of Newtonian inertia, directly encoding the irreversibility of time.

By integrating number theory with statistical physics, the framework yields the unified Microstate-Sequence-Mode-Coupling (MSS-MCT) equations, bridging thermodynamic and dynamic descriptions. The application of this framework simultaneously resolves two long-standing puzzles.

By incorporating the eigen-phase displacement, MSS-MCT achieves quantitative accuracy for the non-Gaussian parameter, correcting the order-of-magnitude underestimation inherent in equilibrium-based mode-coupling theories. The first-principles derivation of the non-Gaussian parameter relation, $\alpha_2(t)$, is pivotal. It not only predicts the correct experimental magnitude ($\sim 1-10$) but fundamentally explains the observed scaling with plateau of $F(q,t)$. Concurrently, the theory delivers a first-principles calculation of the universal polymer constant $C_1=16.7$, closing Flory's conjecture without recourse to the ill-defined concept of free volume.

The quantitative resolution of these two independent benchmarks—one dynamic, one thermodynamic—validates the MSS-MCT equations and confirms the eigen-phase displacement as the precise physical manifestation of the thermodynamic inertia force. This leads to a new conception of a non-equilibrium phase transition: when the eigen-phase displacement exhausts the available free energy, the system's relaxation pathway must change, implying a shift in its reference phase—a profound transition for future energy landscape theories to detail.

In summary, this work validates operationalization of the arrow of time and establishes the resulting thermodynamic inertia as a foundational mesoscopic principle for non-equilibrium matter.

Author Contribution:

Yikun Ren: Conceived and developed the entire theoretical framework of operationalization of the arrow of time, including the foundational concept of eigen-phase displacement and thermodynamic inertia; invented the Microstate Sequence (MSS) theory; derived the thermodynamic inertia force and its semi-group algebra; formulated the unified MSS-MCT equations; performed all formal analysis and analytical derivations; wrote the original manuscript.

Feixiang Xu: Provided resources, assisted in clarifying the operational definition of the degree of non-equilibrium within the proposed framework, assisted with literature review, and contributed to manuscript editing.

Ming Lin: Provided resources and contributed to manuscript editing.

Acknowledge:

Prof. Rui Zhang named the MSS theory. Prof. Liangbin Li supported the whole work. Mr.Xiao Tu helped with the pictures. This work was supported by the National Natural Science Foundation of China (grant number 21973033), the Fundamental Research Funds for Central Universities (grant number 2018ZD13), Jiangxi Provincial Department of Education Project (grant number GJJ2401817), and the China Postdoctoral Science Foundation (grant number 2024M753321).

Reference:

- 1 Binder, K., & Young, A. P. "Spin glasses: Experimental facts, theoretical concepts, and open questions." *Reviews of Modern Physics* 58.4:801-976(1986).
- 2 Cugliandolo, L. F., and J. Kurchan. "Analytical Solution of the Off-Equilibrium Dynamics of a Long Range Spin-Glass Model." *Physical Review Letters* 71.1:173(1993).
- 3 Ediger, M. D., Angell, C. A., & Nagel, S. R.. Supercooled liquids and glasses. *The Journal of Physical Chemistry B.*(1996)
- 4 Evans, D. J., Cohen, E. G. D., & Morriss, G. P. Probability of second law violations in shearing steady states. *Physical Review Letters*, 71(15), 2401-2404(1993).
- 5 Gallavotti, G., & Cohen, E. G. D. Dynamical ensembles in nonequilibrium statistical mechanics. *Physical Review Letters*, 74(14), 2694-2697.(1995)
- 6 Debenedetti, P. G., & Stillinger, F. H. Supercooled liquids and the glass transition. *Nature* 2001, 410(6825), 259–267.
- 7 Angell,C.A. Formation of glasses from liquids and biopolymers. *Science* 267(5206), 1924-1935.(1995)
- 8 Masters, J. R. HeLa cells 50 years on: the good, the bad and the ugly. *Nat. Rev. Cancer* 2, 315–319 (2002).
- 9 Onsager, L. Reciprocal relations in irreversible processes. I. *Phys. Rev.* 37, 405–426 (1931); Onsager, L. Reciprocal relations in irreversible processes. II. *Phys. Rev.* 38, 2265–2279 (1931).
- 10 Prigogine, I. Time, structure, and fluctuations. *Science*, 201 (4358), 777-785.(1978)
- 11 Nicolis, G., & Prigogine, I. *Self-Organization in Nonequilibrium Systems.*(1977)
- 12 Penrose, R. , & Mermin, N. D. The emperor's new mind: concerning computers, minds, and the laws of physics. *American Journal of Physics* 58(12), 1214-1216.(1998)

- 13 Penrose, R. Cycles of time: an extraordinary new view of the universe. *Anuario Filosofico.*(2010)
- 14 Prigogine, I. The end of certainty: time, chaos, and the new laws of nature. *Economics*' in Aerts. (1997)
- 15 Zeh, H. D., The Physical Basis of the Direction of Time. (Springer, Berlin, 1989).
- 16 Hawking, S. W. Arrow of time in cosmology. *Physical review D: Particles and fields*(32)(10), 2489-2495.(1985).
- 17 Lebowitz, J. L. Macroscopic laws, microscopic dynamics, time's arrow and boltzmann's entropy. *Physica A: Statistical Mechanics and its Applications.* (1993)
- 18 Boltzmann, L. Über die Beziehung zwischen dem zweiten Hauptsatze der mechanischen Wärmetheorie und der Wahrscheinlichkeitsrechnung resp. den Sätzen über das Wärmegleichgewicht. *Sitzungsberichte der Kaiserlichen Akademie der Wissenschaften in Wien, Mathematisch-Naturwissenschaftliche Classe* 76, 373–435 (1877).
- 19 Coveney, P. & Highfield, R. The arrow of time: a voyage through science to solve time's greatest mystery. (Fawcett Columbine, New York, 1990).
- 20 Porter, T. "Chapter Seven. TIME'S ARROW AND STATISTICAL UNCERTAINTY IN PHYSICS AND PHILOSOPHY." *The Rise of Statistical Thinking, 1820–1900* (2020).
- 21 Price, H. Time's Arrow and Eddington's Challenge. In *Time: Poincaré Seminar 2010* 115–140 (Birkhäuser, 2013).
- 22 Flenner, E. & Szamel, G. Relaxation in a glassy binary mixture: Comparison of the mode-coupling theory to a Brownian dynamics simulation. *Phys. Rev. E* 72, 031508 (2005).
- 23 Schnyder, S. K. et al. Dynamic heterogeneities and non-Gaussian behavior in two-dimensional randomly confined colloidal fluids. *Phys. Rev. E* 95, 032602 (2017).
- 24 Berthier, L., et al. Non-Gaussian effects in glassy dynamics. *J. Chem. Phys.* 130, 125102 (2009).
- 25 Kim, K. & Yamamoto, R. Non-Gaussian parameter of glass-forming liquids: A molecular dynamics simulation study. *J. Chem. Phys.* 133, 144502 (2010).
- 26 Götze, W. & Sjögren, L. Relaxation processes in supercooled liquids. *Rep. Prog. Phys.* 55, 241–376 (1992).
- 27 Reichman, D. R. & Charbonneau, P. Mode-coupling theory. *J. Stat. Mech.* 2005, P05013 (2005).
- 28 Kubo, R. Statistical Physics II: Nonequilibrium Statistical Mechanics. (Springer-Verlag, 1991).
- 29 Jarzynski, C. Nonequilibrium equality for free energy differences. *Phys. Rev. Lett.* 78, 2690–2693 (1997).
- 30 Crooks, G. E. Entropy production fluctuation theorem and the nonequilibrium work relation for free energy differences. *Phys. Rev. E* 60, 2721–2726 (1999).
- 31 Evans, D. J., Cohen, E. G. D., & Morriss, G. P. Probability of second law violations in shearing steady states. *Phys. Rev. Lett.* 71, 2401–2404 (1993).
- 32 Sevick, E. M., Prabhakar, R., Williams, S. R., & Searles, D. J. Fluctuation theorems. *Annu. Rev. Phys. Chem.* 59, 603–633 (2008).

33 Williams, M. L., Landel, R. F. & Ferry, J. D. The Temperature Dependence of Relaxation Mechanisms in Amorphous Polymers and Other Glass-forming Liquids. *Journal of the American Chemical Society* 77, 3701-3707 (1955).

34 Ferry, J. D. *Viscoelastic Properties of Polymers*. 3rd edn (Wiley, 1980).

35 Cohen, M. H. & Grest, G. S. Liquid-glass transition, a free-volume approach. *Phys. Rev. B* 20, 1077–1098 (1979).

36 Roland, C. M. Characteristic relaxation times and their invariance to thermodynamic conditions. *Soft Matter* 4, 2316–2322 (2008).

37 Angell, C. A. Entropy and fragility in supercooled liquids. *J. Res. Natl. Inst. Stand. Technol.* 102, 171–185 (1997).

38 Simha, R. , & Boyer, R. F. On a general relation involving the glass temperature and coefficients of expansion of polymers. *The Journal of Chemical Physics* 37(5), 1003-1007 (1962).

39 Grest, G. S. & Cohen, M. H. Liquids, Glasses, and the Glass Transition: A Free-Volume Approach. *Adv. Chem. Phys.* 48, 455–525 (1981)

40 Adam, G. & Gibbs, J. H. On the Temperature Dependence of Cooperative Relaxation Properties in Glass-Forming Liquids. *The Journal of Chemical Physics* 43, 139-146 (1965).

41 Angell, C. A. Relaxation in liquids, polymers and plastic crystals — strong/fragile patterns and problems. *J. Non-Cryst. Solids* 131–133, 13–31 (1991).

42 Böhmer, R., Ngai, K. L., Angell, C. A. & Plazek, D. J. Nonexponential relaxations in strong and fragile glass formers. *J. Chem. Phys.* 99, 4201–4209 (1993).

43 Berthier, L. & Biroli, G. Theoretical perspective on the glass transition and amorphous materials. *Rev. Mod. Phys.* 83, 587–645 (2011).

44 Prigogine, I.. "Introduction to thermodynamics of irreversible processes." *Journal of the Electrochemical Society* 1.4(1955).

45 Nicolis, G., & Prigogine, I. *Self-Organization in Nonequilibrium Systems: From Dissipative Structures to Order through Fluctuations.*(1977)

46 Ren, Y., Xu, F., Lin, M. & Hua, Q. Microstate Sequence Theory of Phase Transition: Theory Construction and Application on 3-Dimensional Ising Model. *Fortschritte der Physik* 73, 2300249 (2024).

47 Mori, H. "Transport, Collective Motion, and Brownian Motion." *Progress of Theoretical Physics* 33.3:423-455.(1965)

48 Zwanzig, R. "Ensemble Method in the Theory of Irreversibility." *Journal of Chemical Physics* 33.5:1338-1341.(1960)

49 Mézard M, Parisi G, & Virasoro M. A. *Spin Glass Theory and Beyond: An Introduction to the Replica Method and Its Applications*[M]. Singapore: World Scientific, 1987.

50 Meyer, H., Biroli, G., & Bouchaud, J. P. "Mode-coupling theory as a mean-field description of the glass transition." *Physical Review Letters* 104, 255704 (2010).

51 Prigogine, I. *Introduction to Thermodynamics of Irreversible Processes*. 3rd edn (Wiley-Interscience, 1967).

52 De Groot, S. R. & Mazur, P. *Non-Equilibrium Thermodynamics*. (Dover Publications, 1984).

53 Fodor, É. & Marchetti, M. C. The statistical physics of active matter: From self-catalytic colloids to living cells. *Physica A* 504, 106–120 (2018).

54 Maes, C. *Non-Dissipative Effects in Nonequilibrium Systems*. (Springer, 2018).

55 Janssen, L. M. C., Mayer, P. & Reichman, D. R. Generalized mode-coupling theory of the glass transition. *Phys. Rev. E* 94, 054603 (2016).

56 Götze, W. & Sperl, L. Extended mode-coupling theory. *Phys. Rev. E* 66, 011405 (2002).

57 Zacccone, A. & Terentjev, E. M. Disorder-assisted melting and the glass transition in amorphous solids. *Phys. Rev. B* 88, 174203 (2013).

58 Schweizer, K. S. & Saltzman, E. J. Entropic barriers, activated hopping, and the glass transition in colloidal suspensions. *J. Chem. Phys.* 119, 1181–1196 (2003).

59 Frick, B. & Richter, D. The microscopic basis of the glass transition in polymers from neutron scattering studies. *Science* 267, 1939–1945 (1995).

60 Weeks, E. R., Crocker, J. C., Levitt, A. C., Schofield, A., & Weitz, D. A. Three-Dimensional Direct Imaging of Structural Relaxation Near the Colloidal Glass Transition. *Science* 287, 627–631 (2000).

61 Lu, P. J., et al. Gelation of particles with short-range attraction. *Nature* 453, 499–503 (2008).

62 Flenner, E. & Szamel, G. Relaxation in a glassy binary mixture: Comparison of the mode-coupling theory to a Brownian dynamics simulation. *Phys. Rev. E* 72, 031508 (2005).

63 Zaccarelli, E., et al. Structural and dynamical arrest of attractive colloids: a numerical study. *J. Phys.: Condens. Matter* 14, 2633–2650 (2002).

64 Mattsson, J., et al. Soft colloids make strong glasses. *Nature* 462, 83–86 (2009).

65 Vorselaars, B., Lyulin, A. V., Michels, M. A. J. & Karatasos, K. Non-Gaussian effects in the isotropic phase of a liquid crystal: Comparison of simulation with theory. *Phys. Rev. E* 75, 011504 (2007).

66 Habicht, J., et al. Non-Gaussian nature of glassy dynamics by cage to cage motion. *J. Chem. Phys.* 134, 184508 (2011).

67 Hansen, J. P. & McDonald, I. R. *Theory of Simple Liquids: with Applications to Soft Matter*, (Academic Press, London, 2013).

68 Doi, M. *Introduction to Polymer Physics*, Oxford University Press, Oxford, Great Britain, 1995.

69 Colmenero, J. et al. Inelastic neutron scattering for investigating the dynamics of confined glass-forming liquids. *J. Non-Cryst. Solids* 351, 2657–2667 (2005).

70 Shi, Y. et al. Structural evolution of fused silica below the glass-transition temperature revealed by in-situ neutron total scattering. *J. Non-Cryst. Solids* (2022).

71 Ren Y., Li Y., and Li L., A Theoretical Interpretation of Free Volume at Glass Transition, *Chinese Journal of Polymer Science* 35, 1415-1427(2017).

72 Wunderlich, B. Thermal analysis of polymeric materials. *Thermochimica Acta* 355, 43–57 (2000).

73 Jean, Y. C., et al. Characterization of free volume and density gradients in polymer films using positron annihilation spectroscopy. *Macromolecules* 40, 2522–2530 (2007).

74 Menard, K. P. *Dynamic Mechanical Analysis: A Practical Introduction*. 2nd ed. (CRC Press, 2008).

75 Mangialetto, J., Van den Brande, N., Van Mele, B., & Wübbenhorst, M. Real-Time Determination of the Glass Transition Temperature during Reversible Network Formation Based on Furan–Maleimide Diels–Alder Cycloadditions Using Dielectric Spectroscopy. *Macromolecules*, 56(12), 4727–4737 (2023).

76 Alghannam, E. M. A., Sabanayagam, C. R., Dittrich, P. S., & Isa, L. Molecular rotors to probe the local viscosity of a polymer glass. *J. Chem. Phys.* 156, 174901 (2022).

77 Vrselja, Z. et al. Cellular recovery after prolonged warm ischaemia of the whole body. *Nature* 608, 405–412 (2022).

78 Reichman, D. R. & Charbonneau, P. Mode-coupling theory. *J. Stat. Mech.* 2005, P05013 (2005).